

Photoinduced DNA cleavage by atomic oxygen precursors in aqueous solution†

Cite this: *RSC Advances*, 2013, 3, 12390

James Korang, Ismaila Emahi, Whitney R. Grither, Sara M. Baumann, Dana A. Baum* and Ryan D. McCulla*

Reactive oxygen species are known to induce DNA strand cleavage and have been explored as treatments for cancer. The development of aqueous-soluble dibenzothiophene-*S*-oxide (DBTO) derivatives has made it possible to investigate the mechanism of DNA cleavage by these photoactivatable precursors of atomic oxygen. In addition to the release of atomic oxygen, DBTO can also undergo other processes such as α -cleavage. An objective of this work was to establish whether the extent of strand scission could be attributed to a direct reaction between atomic oxygen and DNA. To accomplish this aim, the extent of strand cleavage upon irradiation of three different DBTO derivatives was measured by the conversion of circular pUC19 plasmid (Form I) to nicked (Form II) as monitored by gel electrophoresis. The interaction of the sulfoxides with DNA was systematically studied by optical melt and fluorescence anisotropy experiments. Thiols are susceptible to rapid oxidation by atomic oxygen, and thus, glutathione was used as a ROS scavenger to determine if DNA cleavage was induced by the release of atomic oxygen. The results from these experiments indicated atomic oxygen was at least partially responsible for the observed strand scission.

Received 7th September 2012,
Accepted 10th May 2013

DOI: 10.1039/c3ra41597j

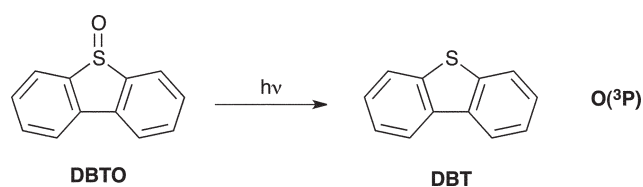
www.rsc.org/advances

Introduction

Despite the known harmful physiological effects of reactive oxygen species (ROS), judicious application of ROS has resulted in many advances in medicine.^{1–3} For example, the combination of light, photosensitizers, and molecular oxygen to generate singlet oxygen ($^1\text{O}_2$) has been employed in photodynamic therapy (PDT), which is an important treatment option for cancer.^{4–6} In PDT, the ability of ROS to oxidatively cleave DNA is used to destroy tumor cells. The hypoxic nature of tumor cells hinders PDT by limiting the photochemical generation of singlet oxygen, which limits the effectiveness of PDT treatments.⁷ In this sense, other light assisted treatments that do not require the presence of molecular oxygen for the generation of ROS would be advantageous.^{8,9} An ideal photoagent for hypoxic tumors would be (1) effective in the absence of molecular oxygen, (2) stable until irradiated, and (3) able to intercalate into DNA. Therefore, a two-component system involving light and a prodrug that can intercalate and generate ROS without the presence of molecular oxygen would be advantageous.

Dibenzothiophene-*S*-oxide (DBTO) undergoes deoxygenation upon irradiation, generating atomic oxygen [$\text{O}(^3\text{P})$] as shown in Scheme 1.^{10–12} Due to inconvenient means of

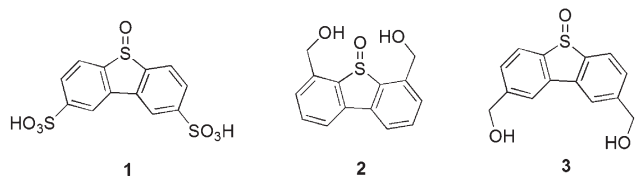
generation, the reactivity of $\text{O}(^3\text{P})$ in solution had not received much attention until DBTO was discovered as an efficient, photoactivatable precursor.^{10–15} Greer and coworkers reported the ability of DBTO to photoinduce the cleavage of plasmid DNA.¹⁶ In their work, it was observed that DNA strand cleavage occurred during irradiation in acetonitrile/water solutions in the absence of molecular oxygen. It was speculated that the photoinitiated DNA strand cleavage by DBTO occurred through $\text{O}(^3\text{P})$ -mediated process. This suggested DBTO had potential as a DNA photocleavage agent that does not require molecular oxygen. Recently, the first aqueous-soluble DBTO derivatives were prepared and a considerable increase in the quantum yield of photodeoxygenation was observed.¹⁷ The increase in quantum yield suggests these derivatives could be efficient DNA photocleavage agents since the extent of DNA cleavage was expected to depend on the quantity of oxidant generated during the photodeoxygenation.



Scheme 1

Department of Chemistry, Saint Louis University, 3501 LaClede Avenue, St. Louis, MO, USA. E-mail: rmccull2@slu.edu; dbaum1@slu.edu

† Electronic supplementary information (ESI) available: UV absorption, fluorescence titration. See DOI: 10.1039/c3ra41597j



Scheme 2

To investigate this hypothesis, the capacity of water-soluble DBTO derivatives, shown in Scheme 2, to photoinduce DNA cleavage was investigated. In order to accomplish this aim, 5-oxodibenzothiophene-2,8-disulfonic acid (**1**) was synthesized and its photochemistry compared to 4,6-hydroxymethyldibenzothiophene *S*-oxide (**2**) and 2,8-hydroxymethyldibenzothiophene *S*-oxide (**3**). The role of O(³P) in the DNA photocleavage induced by these three sulfoxides and the noncovalent interactions between the sulfoxides and the plasmid DNA were investigated.

Materials and methods

Reagents

Commercial materials were obtained from Sigma-Aldrich (St. Louis, MO) or Fischer Scientific (Fair Lawn, NJ) and used without modification, except as noted. Sulfoxides **2** and **3** were prepared as described previously.¹⁷ The sulfoxide **1** was prepared by the following procedure.

Dibenzothiophene-2,8-disulfonic acid (**1S**)

Chlorosulfonic acid (0.5 ml, 7.5 mmol) was added to 40 ml dichloromethane (CH₂Cl₂) at 0 °C. Dibenzothiophene (0.50 g, 2.7 mmol) was added gradually over 15 min. The reaction was stirred for 30 min on ice. The reaction mixture was allowed to warm to room temperature and then allowed to stir for an additional 10 min. The reaction mixture was then placed on ice and the precipitated products were filtered and washed with CH₂Cl₂. The precipitate was dissolved in methanol and passed through silica plug with methanol serving as the eluent to remove salts. The product was recrystallized from water/acetonitrile twice to yield dibenzothiophene-2,8-disulfonic acid (0.19 g, 20% yield). ¹H NMR (400 MHz, DMSO-d): δ 8.397 (d, 2H, *J* = 1.8), 7.995 (d, *J* = 8.2, 2H), 7.775 (dd, *J* = 8.2, *J* = 1.8, 2H), 7.460 (s, 2H) ¹³C NMR (400 MHz, D₂O) δ 142.19, 138.99, 133.98, 123.94, 123.13, 118.75 HRMS (FAB): *m/z* found 342.940, calcd 342.948 (M - H)⁺, M = C₁₂H₈O₆S₃.

5-oxodibenzothiophene-2,8-disulfonic acid (**1**)

Compound **1S** (0.19 g, 0.54 mmol) was dissolved in 95 : 5 methanol/water mixture and cooled to -42 °C. Dimethyldioxirane (DMDO, 0.8 M, 1 eq.) was added dropwise and the reaction monitored by HPLC. When the starting material was totally consumed (~15 min) the reaction was quenched by removing the solvent under reduced pressure. The mixture was purified by preparative HPLC using HASIL 100 C18 5 μm column (0.11 g, 57% yield). Solubility in water

was determined by measuring the octanol water coefficient *K*_{ow} by the shake flask method.^{17,18} The *K*_{ow} for the compound **3** in water was determined to be less than 0.001. ¹H NMR (400 MHz, DMSO): δ 8.132 (d, *J* = 1.2, 2H), 8.053 (d, *J* = 8.0, 2H), 7.803 (dd, *J* = 8.0, *J* = 1.4, 2H), 5.210 (s, 2H) ¹³C NMR (400 MHz, D₂O) δ 147.63, 145.17, 137.20, 128.14, 127.63, 120.30 HRMS (FAB): *m/z* found 358.935, calcd 359.943 (M - H)⁺, M = C₁₂H₈O₇S₃.

Irradiations

The quantum yield measurements were carried out with a 75 W Xe arc lamp focused on a monochromator for wavelength selection. Slit widths allowed ±6 nm of linear dispersion from the set wavelength. Samples (4.8 mL) in a 1 cm quartz cell were placed in a permanently mounted cell holder such that all of the exiting light hit the sample without further focusing. For all direct quantum yield measurements, the concentration of the starting material was confirmed as sufficient to obtain a minimum absorbance of 2 at the selected wavelength, and the samples were irradiated until approximately 15% conversion of the starting material was reached. Analysis of the reaction mixtures at various time points was performed with an HPLC. Photolysis of azoxybenzene to yield the rearranged product, *o*-hydroxyazobenzene, was used as the actinometer.¹⁹

pUC19 plasmid DNA

Plasmid pUC19 DNA was transformed into chemically competent *E. coli* (TOP10 chemically competent *E. coli*, Invitrogen, Carlsbad, CA) following the manufacturer's protocol. Plasmid DNA was isolated from cultured cells using a PerfectPrep Spin Mini kit (5PRIME, Gaithersburg, MD), followed by ethanol precipitation. The concentration of the DNA stock was quantified by UV absorbance using a NanoDrop Spectrophotometer (Thermo Scientific).

DNA photocleavage studies

An aqueous solution containing a mixture of 0.1 mM sulfoxide and 40.0 ng μl⁻¹ pUC19 plasmid DNA was irradiated in fused-silica test tubes at room temperature. A Luzchem LZC-4C photoreactor with broadly emitting fluorescent bulbs centered at 350 nm was used as the irradiation source. All samples were purged with argon or allowed to stand in air for 1 h in the dark prior to irradiation.

Atomic oxygen inhibition studies

A 1X PBS [11.9 mM phosphates (Na₂HPO₄ and KH₂PO₄), 137 mM NaCl, 2.7 mM KCl, pH 7.0] buffer solution containing 0.1 mM sulfoxide and varying glutathione (GSH) concentrations was irradiated together with 40.0 ng μl⁻¹ pUC19 plasmid DNA in fused-silica test tubes in a Luzchem LZC-4C photoreactor using broadly emitting fluorescent bulbs centered at 350 nm.

DNA photocleavage analysis

After photolysis, 20 μL of the irradiated solution was analyzed by agarose gel electrophoresis. Products were separated on a 1% agarose gel using 1X TAE (40 mM Tris-acetate, 1 mM EDTA, pH 8.0) running buffer. The conversion of uncut supercoiled pUC19 plasmid DNA (Form I) to its nicked (Form II) was visualized by ethidium bromide staining. Once

electrophoresis had been done, all the stained gels were photographed using a FOTODYNE Gel Documentation system equipped with a FOTO/UV 26 dual light transilluminator. The intensity of the bands were analyzed using the ImageQuantTL software package (GE Healthcare). The band percentage corresponding to the amount of Form I or Form II was obtained.

Optical melting studies

The ability of sulfoxides **1–3** to bind to DNA was studied by conducting optical melting experiments using the sulfides **1S–3S** since they are not photoactive. Four different DNA duplexes were used for the melt studies. Each duplex consisted of 12 base pairs with constant stem sequences of GGTGXXXXTGG/CCACZZZZCACC on either side of a varied 4 base-pair sequence. Each DNA duplex was melted in the presence and absence of the sulfides to determine changes in the melting temperature (ΔT_M). The melt experiments were performed in melt buffer (1 M NaCl, 20 mM sodium cacodylate, 0.5 mM EDTA, pH 7.0). HPLC-purified DNA oligonucleotides were obtained from Integrated DNA Technologies (IDT, Coralville, IA) and used to prepare the DNA duplexes. The 1 : 1 ratio of 50 μM sulfide and DNA duplex were placed in quartz cuvettes (0.1 cm). The absorbance at 260 nm was continuously monitored for the DNA duplex solution in the absence and presence of the sulfide whilst increasing the temperature from 25 $^\circ\text{C}$ to 95 $^\circ\text{C}$ at a rate of 0.5 $^\circ\text{C min}^{-1}$ using a Beckman Coulter DU 800 spectrophotometer equipped with a Beckman-Coulter high performance temperature controller. Data analysis was performed with MeltWin[®] 3.5 software, which was used to calculate the first derivative of the $\Delta A_{260}/\Delta T$ vs. temperature. The melting temperature, T_M , value for each melting isotherm was determined by finding the maximum of the first derivative plot obtained by plotting $\Delta A_{260}/\Delta T$ vs. temperature.²⁰

Fluorescence anisotropy studies

To further investigate the ability of the sulfoxide compounds **1–3** to bind to DNA, fluorescence anisotropy measurements were carried out using a Fluorolog 3 fluorometer (Horiba Scientific, Edison, NJ). For each compound, a 100 μM solution of the compound was made in 150 μL of 1X PBS buffer. This solution was transferred into a cuvette and the anisotropy value recorded. Additional solutions containing 100 μM of the sulfoxide compound with different DNA concentrations (5, 10, 25, and 50 $\text{ng } \mu\text{L}^{-1}$) were prepared similarly and anisotropy values measured. All anisotropy measurements were done at an excitation wavelength of 290 nm and an emission wavelength of 387 nm. The excitation bandpass was set to 19 and signals were taken at 9800 counts per second (cps). Measurements were taken three times at each DNA concentration, with an integration time of 10 s, and the resulting anisotropy values were averaged.

Results and discussion

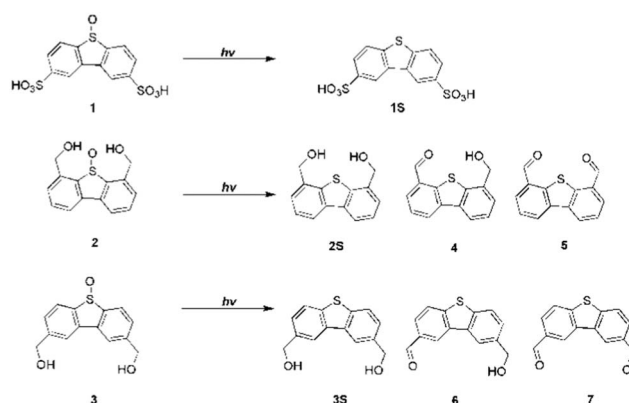
Photoactivatable $\text{O}(^3\text{P})$ precursors

The sulfoxides **2** and **3** were synthesized as reported in literature.¹⁷ Sulfoxide **1** was synthesized by sulfonation of

dibenzothiophene using chlorosulfonic acid, and the resulting DBT was oxidized to DBTO with DMDO. Hydrophilicity was gauged by the octanol/water coefficient K_{ow} which was obtained experimentally using the shake-flask method.²¹ A solution of 8-octanol (5 mL) and water (5 mL) were allowed to come to a saturation equilibrium overnight. 2–3 mmol of the desired compound was added to the solution in a capped test tube. The solution was continuously inverted over the period of 1 h and then centrifuged to eliminate emulsion. The octanol and water layers were then separated, and concentration of compound in each layer was assessed by HPLC.¹⁷ The value of K_{ow} for the sulfoxides were less than 0.001, 2.55 and 1.88 for **1**, **2** and **3** respectively. These values indicates the aqueous solubility of **1** is significantly higher than **2** and **3**. In general, these DBTO derivatives are very soluble in water compared to DBTO with $K_{ow} = 78$, which was also determined by the shake-flask method.

Quantum yield and photoproducts

Measurements of the quantum yields of photodeoxygenation were performed in water at room temperature. The resulting photoproducts for **1–3** are shown in Scheme 3. The photodeoxygenation of sulfoxides **2** and **3** to generate $\text{O}(^3\text{P})$ were investigated previously.¹⁷ Irradiation of **2** and **3** was reported to produce other photoproducts in addition to the expected deoxygenation photoproducts **2S** and **3S**, respectively. These other photoproducts **4** and **5** for **2** and **6** and **7** for **3** were found to be as a result of oxidation of the hydroxymethyl substituent used to improve the aqueous solubility. Self-oxidation of the side-chains of **2** and **3** necessarily reduced the amount of $\text{O}(^3\text{P})$ being released. The sulfonic acid-substituted precursor **1** was expected to have improved solubility and be resistant to oxidation by $\text{O}(^3\text{P})$. As expected, the irradiation of **1** gave only a single photoproduct **1S**. The quantum yields for the consumption of **1** and the formation of **1S** were determined using azoxybenzene as the actinometer.¹⁹ Quantum yields for the photodeoxygenation reactions of **1–3** are shown in Table 1. The difference between the quantum yields for deoxygenation of **1** and the formation of **1S** were not significant, which was consistent with the expectation that **1** would be less susceptible to oxidation. The significant difference between the quantum yields of deoxygenation for sulfoxides **2** and **3**



Scheme 3

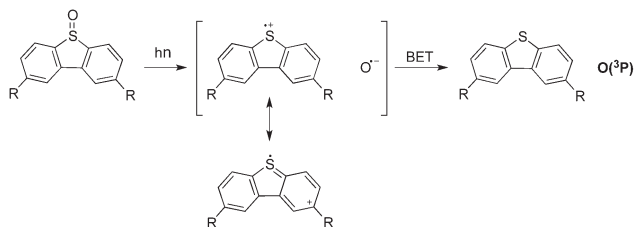
Table 1 Quantum yields for the photodeoxygenation of DBTO derivatives **1–3**^a

Sulfoxides	λ (nm)	Φ_{-DBTO}	Φ_{+DBT}
1	254	0.009 ± 0.003^b	0.004 ± 0.002
1	294	0.018 ± 0.001	0.011 ± 0.005
1	330	0.022 ± 0.009	0.019 ± 0.001
2 ^c	330	0.075 ± 0.020	0.016 ± 0.003
3 ^c	330	0.061 ± 0.001	0.016 ± 0.009

^a Quantum yields for the deoxygenation of the sulfoxide (Φ_{-DBTO}) and the formation of the deoxygenated product (+DBT) determined in aqueous solution. ^b Error reported as 95% confidence interval. ^c Data taken from ref. 17.

compared with the quantum yields of formation of **2S** and **3S** was consistent with a fraction of the oxidant being trapped by the side chains.

The quantum yields for the DBTO derivatives in water were higher than that reported for DBTO ($\Phi_{+DBT} \sim 0.003$) in organic media.^{14,15} In organic solvents, the posited primary deoxygenation mechanism for DBTO is the unimolecular S–O bond cleavage leading to the sulfide and O(³P) from the first singlet excited state of DBTO.^{11,15,17,22,23} The increase in quantum yield of photodeoxygenation in low or neutral pH water was suggested to arise from the increased polarity of the solvent.¹⁷ The polar solvent was postulated to stabilize charge separation during the cleavage of S–O bond, leading formally to an oxygen atom radical anion and a DBT radical cation, prior to favorable back electron transfer (BET) leading to the formation of O(³P) and the sulfide. Thus, the significant increase in deoxygenation quantum yields in aqueous media was suggested to result from the water assisting in separating the charges formed during bond cleavage compared to organic solvents. The differences in deoxygenation quantum yields (Φ_{-DBTO}) between **1–3** are consistent with the expected substituent effects for the proposed mechanism. As shown in Scheme 4, an increase of a positive charge on sulfur of the dibenzothio- phene moiety would be expected to delocalize to the 2 and 8 positions. The electron withdrawing sulfonic acid substituent would destabilize the dibenzothio- phene cation radical and concomitantly lower the quantum yield of deoxygenation. Likewise, the hydroxymethyl substituents would be expected to stabilize the positive charge, which is consistent with the higher quantum yields for deoxygenation **2** and **3** compared to **1**.

**Scheme 4**

DNA photocleavage

The ability of **1–3** to photochemically cleave DNA was investigated in aqueous media at room temperature. The photoinduced DNA cleavage by DBTO derivatives was monitored using gel electrophoresis by measuring the conversion of supercoiled pUC19 plasmid DNA (Form I) to nicked circular DNA (Form II), which occurs upon a single strand scission. In these experiments, aqueous solutions containing supercoiled plasmid DNA and the sulfoxide of interest were irradiated at room temperature in a Luzchem LZC-4C photoreactor using broadly emitting fluorescent bulbs centered at 350 nm. Irradiations were performed under both aerobic and anaerobic conditions. From a representative experiment, Fig. 1 depicts the gels obtained for the irradiation of pUC19 plasmid DNA and a sulfoxide (**1–3**) under aerobic conditions. The figure clearly shows a substantial decrease in the band percent of Form I from 90% to between 40–15% for all three DBTO derivatives. Similar results were obtained under anaerobic condition. Anaerobic conditions were achieved by degassing the samples through argon sparging for 15 min. The decrease in percent band for Form I confirmed the ability of **1–3** to photoinduce DNA cleavage in aqueous solutions at low concentrations. The extent of strand scission increases with time and was consistent with other DNA cleavage agents.^{24,25} In control experiments, no significant increase in Form II was observed when **1–3** were replaced by their corresponding sulfides (**1S–3S**).

For all the experiments, a small percentage of nicked circular DNA was present even prior to photolysis. Additionally, a small (<10%) variable increase in the percent of Form II was observed in control samples that were irradiated but contained no DBTO derivatives. A means to account for these variables was needed. Thus, the following normalization procedure was adopted: the normalized percent change of Form II (N) in control and sample was calculated by dividing the change in band percent before and after irradiation ($\%Form II_{+hv} - \%Form II_{-hv}$) and dividing by the amount of Form I prior to irradiation ($\%Form I_{-hv}$) as shown in eqn (1).

$$N = \left(\frac{\%Form II_{+hv} - \%Form II_{-hv}}{\%Form I_{-hv}} \right) \times 100 \quad (1)$$

$$DNA \text{ Cleavage} = N_{\text{sample}} - N_{\text{control}} \quad (2)$$

The extent of DNA cleavage that could be attributed to the irradiation of **1–3** obtained from the difference between sample (with **1–3**) and control (no **1–3**) using eqn (2). The physical and photochemical properties of the **1–3** are compared to the extent of DNA cleavage caused by the irradiation of these DBTO derivatives is reported in Table 2. The DNA cleavage values reported in Table 2 were obtained from a minimum of five experiments represented by Fig. 1. For **1–3**, the DNA cleavage values in aerobic and anaerobic conditions ranged from 46% to 61% with 95% confidence intervals of approximately $\pm 5\%$. Thus, significant differences

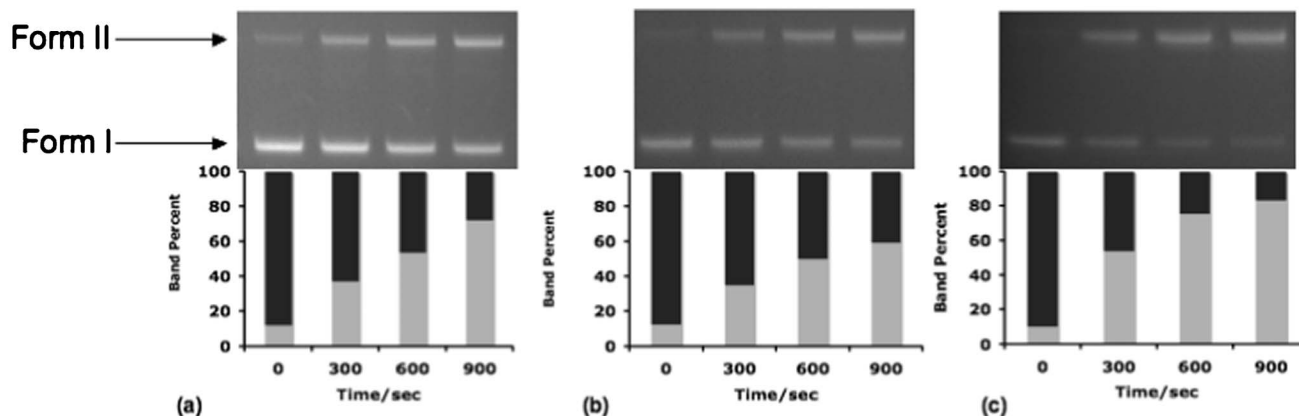


Fig. 1 Time-dependent conversion of supercoiled plasmid pUC19 DNA (Form I) to nicked circular DNA (Form II) in aerobic condition monitored with gel electrophoresis in the presence of (a) compound 1 (b) compound 2 and (c) compound 3 at 0, 300, 600 and 900 s in aqueous media. The concentration of the sulfoxides was kept at 0.1 mM and the plasmid DNA was $40.0 \text{ ng } \mu\text{l}^{-1}$. The gels were imaged and analyzed using ImageQuantTL from which the band percent of Form I to Form II were obtained.

between the values of DNA cleavage photoinduced by **1–3** in anaerobic and aerobic conditions were very small. While the data weakly indicated **3** was the most effective at photoinducing DNA cleavage, a more general conclusion that the extent of photoinduced DNA cleavage was similar for all three DBTO derivatives seems more prudent in the absence of more experiments with other DNA examples.

Hydrophilicity, as gauged by K_{ow} , increased significantly for **1** compared to **2** and **3**. However, the extent of photoinduced plasmid DNA cleavage by **1–3** derivatives remained the same. Thus, no correlation between the hydrophilicity of the $O(^3P)$ -precursors and the extent of photoinduced DNA cleavage was observed. If all of the oxidant generated led to DNA cleavage, then the quantum yield of photodeoxygenation (Φ_{-DBTO}) would be expected to correlate with the extent of DNA cleavage. However, the quantum yield for the photodeoxygenation of the sulfoxides **2** and **3** in aerobic conditions (0.049 and 0.027, respectively) were higher than for **1** (0.011). Likewise, significantly different quantum yields of photodeoxygenation for **1**, **2** and **3**, (0.022, 0.075 and 0.061 respectively) were observed in anaerobic conditions, and yet, similar amounts of DNA cleavage were observed upon irradiation with **1–3**. Thus, no correlation between Φ_{-DBTO} and the extent of photoinduced DNA cleavage by DBTO was observed. For **2** and **3**, it

was expected that some of the oxidant would be lost through internal oxidation of the substituents. Thus, the quantum yield for the formation of the sulfide (Φ_{+DBT}) can be used to represent the amount of escaping oxidant. Both the extent of DNA cleavage and the quantum yield of sulfides formation were similar for **1–3**, which indicated only the escaped $O(^3P)$ led to DNA cleavage. The quantum yields of sulfide formation were higher under anaerobic compared to aerobic condition for the three sulfoxides. Larger quantum yields in anaerobic conditions were expected since molecular oxygen is an efficient quencher of both singlet and triplet excited states. However, it should be noted that no indication of singlet oxygen generation was observed previously.¹⁷ Molecular oxygen is known to enhance intersystem crossing, which would inhibit deoxygenation, without singlet oxygen formation.^{15,26} Thus, the similarities in DNA cleavage under both aerobic and anaerobic conditions might be accounted for by the generation of ozone in aerobic condition. The generation of ozone from $O(^3P)$ and O_2 is a well-known process and ozone was observed during the photodeoxygenation previously.¹⁷

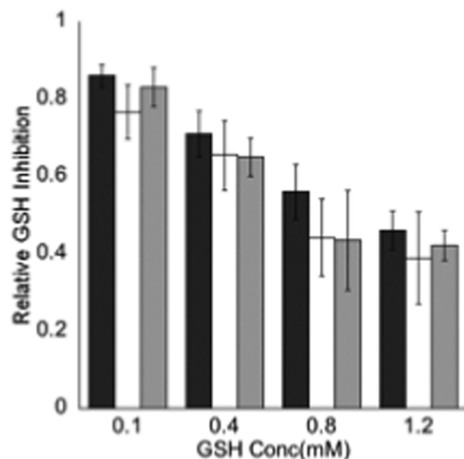
To assess if the observed DNA cleavage was the result of direct oxidation by $O(^3P)$, the photoinduced plasmid DNA cleavage was performed in the presence of the glutathione (GSH). Glutathione is a common ROS scavenging antioxidant,

Table 2 Summary of results of solubility, quantum yields and DNA photocleavage of sulfoxides **1–3** in aqueous media^a

Sulfoxide	K_{ow}	Φ_{-DBTO}^b		Φ_{+DBT}^b		DNA Cleavage ^c	
		Aerobic	Anaerobic	Aerobic	Anaerobic	Aerobic	Anaerobic
1	0.001	0.011 ± 0.006	0.022 ± 0.009	0.009 ± 0.006	0.019 ± 0.001	54 ± 6	47 ± 7
2	1.88	0.049 ± 0.001	0.075 ± 0.002	0.008 ± 0.003	0.016 ± 0.003	46 ± 3	58 ± 2
3	2.55	0.027 ± 0.006^d	0.061 ± 0.001	0.009 ± 0.005	0.016 ± 0.009	58 ± 6	61 ± 6

^a The solubility of the sulfoxides was determined using octanol/water partition coefficient K_{ow} . ^b Quantum yields for the consumption of the sulfoxide ($-DBTO$) and formation of the deoxygenation product ($+DBT$) were determined in aqueous solution in both aerobic and anaerobic conditions at 330 nm. ^c The DNA cleavage data was obtained by normalizing the test result with the control experiment. ^d 95% confidence interval for at least 5 experiments.

(a)



(b)

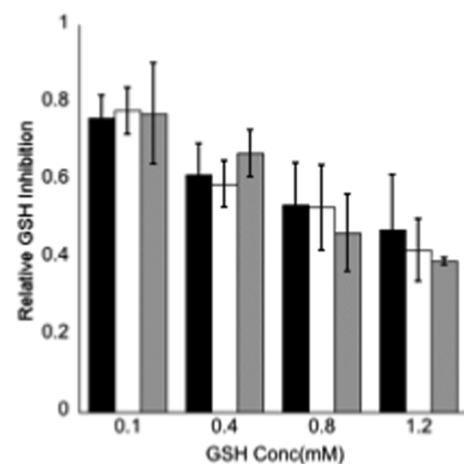


Fig. 2 Glutathione (GSH) inhibition of photoinduced plasmid pUC19 DNA cleavage under both (a) anaerobic and (b) aerobic conditions is shown in bars: sulfoxide **1** (dark grey), **2** (white) and **3** (light grey) was performed in 1X PBS buffer to maintain a pH of 7.0 during irradiation. The concentration of glutathione was increase from 0.1 mM to 1.2 mM whilst keeping the concentration of **1–3** and plasmid DNA constant at 0.1 mM and 40 ng μL^{-1} . The anaerobic condition was obtained by bubbling Argon in the solution for 15 min in the quartz test-tube. 95% confidence level for at least 5 experiments is reported as the error.

and thiols were shown to be susceptible to oxidation by $\text{O}(\text{}^3\text{P})$.^{17,27,28} Thus, GSH was expected to act as a competitive trap for $\text{O}(\text{}^3\text{P})$, and thus, increasing concentrations of GSH were expected to inhibit the photoinduced plasmid DNA cleavage by DBTO derivatives if $\text{O}(\text{}^3\text{P})$ was directly involved. The photoinduced DNA cleavage experiment was performed in the presence of GSH in 1X PBS buffer under both aerobic and anaerobic conditions. The buffer was used to prevent DNA cleavage which occurred upon irradiation if GSH was added without a buffer. In aerobic conditions, the combination of O_2 with $\text{O}(\text{}^3\text{P})$ to form ozone was expected and under anaerobic condition, the only oxidative species expected was $\text{O}(\text{}^3\text{P})$.¹⁷ The ratio of the DBTO derivative and GSH concentration was varied from 1 : 1 to 1 : 12. In Fig. 2, bar graphs of the relative

inhibition of photoinduced plasmid DNA cleavage by GSH for **1–3** under both aerobic and anaerobic conditions are shown. A decrease in DNA cleavage was observed with increasing GSH concentration suggesting an escaping oxidant from **1–3** was involved in the photoinduced plasmid DNA cleavage. However, at GSH concentrations higher than 1.2 mM, there was no further significant inhibition of DNA cleavage, which indicated other reaction mechanisms of **1–3** photolysis apart from that involving $\text{O}(\text{}^3\text{P})$ may also induce DNA strand scission. The products of GSH oxidation may lead to DNA cleavage, however, no DNA cleavage was observed in control experiments using GSH alone in buffered solutions. Another possibility was that noncovalent interaction between the DNA and dibenzothiophene *S*-oxide derivatives prevented GSH from intercepting the oxidant. In order to determine whether a noncovalent interaction plays a role in photoinduced cleavage of DNA by **1–3**, we directed our efforts to investigating the interactions between the sulfoxides and DNA.

DNA binding studies

The photoinduced DNA cleavage by dibenzothiophene *S*-oxide derivatives correlated with the generation of $\text{O}(\text{}^3\text{P})$ as measured by the formation of the sulfide ($\Phi_{+\text{DBT}}$). However, the inability to completely inhibit DNA cleavage at high GSH concentration was possibly due to noncovalent interaction between the DNA and the DBTO derivatives, which would allow $\text{O}(\text{}^3\text{P})$ to react rapidly with the bound DNA thereby preventing scavenging by GSH. Molecules that intercalate with DNA are often planar aromatic heterocycles. Thus, the ability of **1–3** to intercalate with DNA was investigated. Investigation of the intercalation of the DBTO derivatives was performed using optical melt studies. DNA melt studies provide insight into the extent a compound helps stabilize a DNA duplex through non-covalent binding. Specifically, ΔT_{M} gives information as to how well the compound stacks within the base pairs. A positive ΔT_{M} value for DNA duplex in the presence of a molecule indicates the molecule helps stabilize the DNA duplex by binding noncovalently to the DNA duplex. In the optical melt experiment, the corresponding sulfides (**1S–3S**) of **1–3** were used to prevent interference from deoxygenation of the sulfoxide during the melt studies. Four different DNA duplexes in melt buffer solution were used for the melt studies. As shown in Table 3, most of the ΔT_{M} 's were within experimental error of zero, indicating there was no intercalation between the DNA duplexes and the sulfides analogs.

Table 3 ΔT_{M} of the sulfide-duplex equilibria

DNA 12-mer ^a	1S ^b	2S ^b	3S ^b
AAAA/TTTT	-0.87 ± 0.33	-0.15 ± 0.58	-0.07 ± 0.60
ATAT/TATA	0.32 ± 0.46	-0.12 ± 1.41	-0.18 ± 1.28
GGGG/CCCC	-0.27 ± 0.49	-0.13 ± 0.85	0.26 ± 1.43
GCGC/GCGC	-0.01 ± 2.36	-0.26 ± 2.17	-1.31 ± 2.63

^a Nucleotides (X)₄/(Z)₄ within (GGTG(X)₄GTGG)/d(CCAC(Z)₄CACC) overall 12-mer DNA duplex. ^b The corresponding sulfide of the sulfoxides were use to prevent photodeoxygenation during the melt studies.

To further confirm that the three sulfoxides do not intercalate with DNA, UV absorption and fluorescence titrations were used to determine if DNA binding was possible.^{29,30} The spectra of the sample would be expected to change as the amount of plasmid pUC19 increased if the sulfoxides were intercalating. The data from both fluorescence and absorbance titration experiments of 1–3 with plasmid pUC19 are reported in the ESI.† The increasing concentration of plasmid DNA in both the UV absorption and fluorescence titrations resulted in no change in the spectra of the sample, again indicating the sulfoxides do not intercalate into DNA.

While the optical melt and titrations experiments indicated there was no intercalation of 1–3, other modes of noncovalent binding were still possible. To rule out other noncovalent interactions, fluorescence anisotropy was employed to study if 1–3 interact with the pUC19 plasmid. Fluorescence anisotropy is based on the concept that when a molecule binds to another molecule which is fluorescent, the binding event causes a change in the anisotropy of the fluorescing molecule. The technique has been used largely to study protein–DNA binding interactions, in which case the DNA is usually labeled with a fluorophore.³¹ Binding of the protein to the DNA causes an increase in the size of the protein–DNA complex. This subsequently leads to an increased rotational correlation time and therefore anisotropy of the complex compared to that of the free or unbound DNA. In this study, binding of the sulfoxides to the DNA is monitored by change in anisotropy of the sulfoxide compounds. As shown in Fig. 3, there is no significant change in the anisotropy of the sulfoxides 1, 2, and 3 with increasing concentration of DNA, suggesting that they do not bind. This ruled out the possibility of a noncovalent interaction preventing the inhibition of DNA cleavage by GSH. This suggests another mechanism in addition to direct cleavage of DNA by O(³P) must account for the some of the observed cleavage in the presence of a ROS scavenger.

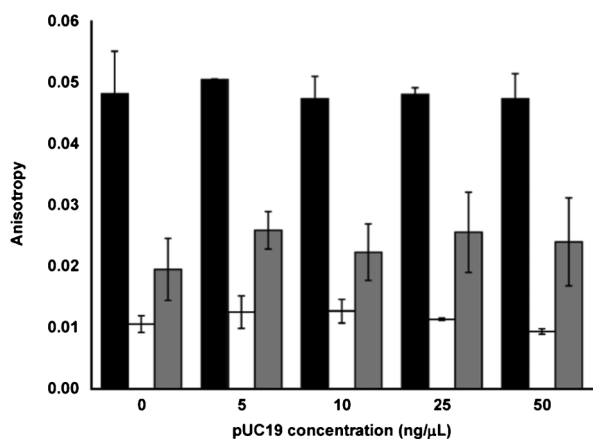


Fig. 3 Fluorescence anisotropy studies of sulfoxides interaction with pUC19 plasmid DNA. Anisotropy was monitored at excitation wavelength of 290 nm and emission wavelength of 387 nm for all three compounds. Measurements were taken three times at each DNA concentration, with an integration time of 10 s, and the resulting anisotropy values were averaged. Standard deviations are approximately ± 0.004 (or less) anisotropy unit.

Aromatic sulfoxides are known to undergo α -cleavage of C–S bond leading to biradicals.³² Studies by other researchers have proposed the biradical as a means of DNA cleavage through H-abstraction.³³ It is unknown if the addition of GSH would significantly inhibit DNA cleavage by these biradicals, and therefore, it is possible to speculate that the biradical from the α -cleavage of the DBTO derivatives 1, 2, and 3 may be involved in the observed DNA cleavage.

Conclusions

In summary, we find that the aqueous soluble DBTO derivatives effectively cleave DNA photochemically in aqueous media. The quantum yields for photodeoxygenation of the these sulfoxides are higher compared to DBTO in organic solvents. The extent of DNA photocleavage correlates well with the quantum yields for the formation of the corresponding sulfides, which indicates DNA cleavage was induced by an escaped oxidant from the photodeoxygenation of DBTO derivatives. The inhibition of DNA photocleavage in the presence of glutathione indicated that atomic oxygen O(³P) plays a role in the DNA cleavage abilities of 1–3. However, another mechanism in addition to the release of O(³P) must account for some of the cleavage since high concentrations of glutathione could not completely inhibit DNA cleavage. The three aqueous soluble dibenzothiophene-S-oxides do not bind to DNA as confirmed by UV melt and fluorescence anisotropy studies.

Acknowledgements

The authors thank Dr. Brent Znosko and the Znosko research group for assistance with the optical melt studies and Dr. Tomasz Heyduk for assistance with the fluorescence anisotropy studies. Portions of this material is based upon work supported by the National Science Foundation under CHE-1255270. The authors thank the National Science Foundation for support under grant CHE-0963363 for renovations to the research laboratories in Monsanto Hall. This work was additionally supported by donors to the Herman Frasch Foundation.

References

- 1 K. Bedard and K. H. Krause, *Physiol. Rev.*, 2007, **87**, 245–313.
- 2 A. L. Garner, C. M. St. Croix, B. R. Pitt, G. D. Leikauf, S. Ando and K. Koide, *Nat. Chem.*, 2009, **1**, 316–321.
- 3 K. M. Kadish, Z. P. Ou, J. G. Shao, C. P. Gros, J. M. Barbe, F. Jerome, F. Bolze, F. Burdet and R. Guillard, *Inorg. Chem.*, 2002, **41**, 3990–4005.
- 4 S. V. Kovalenko and I. V. Alabugin, *Chem. Commun.*, 2005, 1444–1446.
- 5 J. P. Celli, B. Q. Spring, I. Rizvi, C. L. Evans, K. S. Samkoe, S. Verma, B. W. Pogue and T. Hasan, *Chem. Rev.*, 2010, **110**, 2795–2838.

- 6 Y. Huang, Y. Zhang, J. Zhang, D. W. Zhang, Q. S. Lu, J. L. Liu, S. Y. Chen, H. H. Lin and X. Q. Yu, *Org. Biomol. Chem.*, 2009, **7**, 2278–2285.
- 7 B. Breiner, K. Kaya, S. Roy, W. Y. Yang and I. V. Alabugin, *Org. Biomol. Chem.*, 2012, **10**, 3974–3987.
- 8 J. S. Daniels and K. S. Gates, *J. Am. Chem. Soc.*, 1996, **118**, 3380–3385.
- 9 J. S. Daniels, T. Chatterji, L. R. MacGillivray and K. S. Gates, *J. Org. Chem.*, 1998, **63**, 10027–10030.
- 10 A. B. Thomas and A. Greer, *J. Org. Chem.*, 2003, **68**, 1886–1891.
- 11 M. Nag and W. S. Jenks, *J. Org. Chem.*, 2004, **69**, 8177–8182.
- 12 R. D. McCulla and W. S. Jenks, *J. Am. Chem. Soc.*, 2004, **126**, 16058–16065.
- 13 J. C. Scaiano, G. Bucher, M. Barra, D. Weldon and R. Sinta, *J. Photochem. Photobiol., A*, 1996, **102**, 7–11.
- 14 Z. H. Wan and W. S. Jenks, *J. Am. Chem. Soc.*, 1995, **117**, 2667–2668.
- 15 D. D. Gregory, Z. H. Wan and W. S. Jenks, *J. Am. Chem. Soc.*, 1997, **119**, 94–102.
- 16 O. R. Wauchope, S. Shakya, N. Sawwan, J. F. Liebman and A. Greer, *J. Sulfur Chem.*, 2007, **28**, 11–16.
- 17 J. Korang, W. R. Grither and R. D. McCulla, *J. Am. Chem. Soc.*, 2010, **132**, 4466–4476.
- 18 R. Kowalewski and P. Margaretha, *Helv. Chim. Acta*, 1993, **76**, 1251–1257.
- 19 S. P. Vaish, J. LaMarre and N. J. Bunce, *Photochem. and Photobiol.*, 1984, **39**, 531.
- 20 P. L. Vanegas, T. S. Horwitz and B. M. Znosko, *Biochemistry*, 2012, **51**, 2192–2198.
- 21 A. Leo, C. Hnasch and D. Elkins, *Chem. Rev.*, 1971, **71**, 525–616.
- 22 K. Kumazoe, K. Arima, S. Mataka, D. J. Walton and T. Thiemann, *J. Chem. Res.*, 2003, 60–61.
- 23 E. Lucien and A. Greer, *J. Org. Chem.*, 2001, **66**, 4576–4579.
- 24 M. M. Gonzalez, M. Pellon-Maison, M. A. Ales-Gandolfo, M. R. Gonzalez-Baro, R. Erra-Balsells and F. M. Cabrerizo, *Org. Biomol. Chem.*, 2010, **8**, 2543–2552.
- 25 C. A. Terry, L. Gude, M. J. Fernandez, A. Lorente and K. B. Grant, *Bioorg. Med. Chem. Lett.*, 2011, **21**, 1047–1051.
- 26 C. S. Parmenter and J. D. Rau, *J. Chem. Phys.*, 1969, **51**, 2242–2246.
- 27 K. Bahrami, *Tetrahedron Lett.*, 2006, **47**, 2009–2012.
- 28 J. F. Turrens, *J. Physiol.*, 2003, **552**, 335–344.
- 29 M. Aslanoglu and N. Oge, *Turk. J. Chem.*, 2005, **29**, 477–485.
- 30 B. Rajendar, Y. Sato, S. Nishizawa and N. Teramae, *Bioorg. Med. Chem. Lett.*, 2007, **17**, 3682–3685.
- 31 T. Heyduk and J. C. Lee, *Proc. Natl. Acad. Sci. U. S. A.*, 1990, **87**, 1744–1748.
- 32 Y. Guo and W. S. Jenks, *J. Org. Chem.*, 1997, **62**, 857–864.
- 33 A. G. Myers, S. B. Cohen and B. M. Kwon, *J. Am. Chem. Soc.*, 1994, **116**, 1670–1682.